Analytical Estimation of Stress-Induced Birefringence in Panda-Type Polarization-Maintaining Fibers

Junhao Liu, Yifan Liu, and Tianhua Xu, *Member, IEEE*

***Abstract*—An analytical model for estimating the stress-induced birefringence in true Panda-type polarization-maintaining fibers with imperfect geometry has been developed in this letter. The developed model is simpler and more accurate compared to conventional sophisticated and asymptotic formulas in reported works. Our model provides a clear and simple solution to demonstrate the periodic dependence of the birefringence on the misalignment angle between the two stress-applying parts, and the monotonic dependence on the geometric parameters of stress-applying parts. Our work also reveals the important role of the misalignment angle between the two stress-applying parts in practical Panda-type fibers.**

***Index Terms*—Panda-type fibers, Polarization-maintaining optical fibers, Stress-induced birefringence.**

I. Introduction

THE intrinsic stress-induced birefringence (SIB) in polarization-maintaining optical fibers (PMFs) is one of the most crucial characteristics in several applications, e.g. fiber optic sensing [1], loop mirror [2], current transformers [3], acoustic-optic modulators [4] and gyroscopes [5]. The SIB in PMFs originates from the stress difference between two principal axes, produced by embedded stress-applying parts (SAPs) via the difference between the coefficient of thermal expansion (CTE) in SAPs and that in the fiber cladding [6]. It was reported that the SIB can be estimated using the thermo-elastic displacement potential (TEDP) [7], [8], the infinite small element [9] and the finite element method (FEM) [10]-[12] based on TEDP. The TEDP method has wide applications [13] and has recently been used in analyzing single-hole PMFs [14]. However, results of pioneering works in [7] and [8] based on TEDP do not match each other, even for the most commonly applied standard Panda-type PMFs, which have the simplest shape of circular SAPs. This is because the birefringence and stresses were calculated in the rectangular and the polar coordinate systems, separately. The disagreement originates from the transformation between coordinate systems. There are two normal stress components in the polar system: σ_ρ in the radial direction and σ_θ in the circumferential direction. Both contribute to the two principal stresses σ_x and σ_y in the rectangular coordinate system [15], leading to the generation of the SIB. Analyses in [7] utilized the first component only and underestimated the birefringence. Derivations in [8] employed both components, but confused the polar angle in the polar coordinate system with the angle between the two coordinate systems, even for ideal Panda-type PMFs. Nevertheless, the overestimation model in [8] was extensively applied in the calculation of SIB, e.g. FEM [16] and analytical method [13]. In this letter, the model of the SIB in generally asymmetric PMFs is reinvestigated based on the TEDP approach, while all stress components (two produced by each SAP) in the polar system are considered and a proper coordinate transformation are applied. A simpler and more accurate analytical model is obtained for estimating the SIB in PMFs, compared to sophisticated and asymptotic formulas reported in [7] and [8] for PMFs with symmetry about slow axis. The discrepancy between the model in [7] and that in [8] have also been solved. Meanwhile, the developed model can evaluate SIBs in both symmetric and asymmetric PMFs. It can also be used to explain the dependency of SIB on the parameters of SAPs, especially the misalignment angle between two SAPs in Panda-type PMFs. Our model provides a convenient and accurate solution for estimating the birefringence in the design and analysis of PMFs.

Manuscript received ; revised ; accepted . Date of publication ; date of current version .

(Corresponding author: Junhao Liu and Tianhua Xu).

J. Liu is with Tianjin Electronic Materials Research Institute, Tianjin, 300220, China (e-mail: uceexux@ucl.ac.uk). Y. Liu and T. Xu are with University of Warwick, Coventry, CV4 7AL, UK (e-mail: tianhua.xu@ieee.org). T. Xu is also with Tianjin University, Tianjin 300072, China and University College London, London, WC1E 6BT, UK.

II. Theoretical Model

Early works investigated the SIB in Panda-type PMFs, symmetrical about x-axis, as shown in Fig. 1(a). The SIB was described with a polar angle θ by Eq. (32) in [8] and a subtended angle 2ϕ by Eq. (19) in [7]. To provide a generic analysis, a Panda-type PMF with an asymmetric transverse cross section is considered in Fig. 1(b). The core and the cladding are concentric circles centered at O with radii of a and b, respectively. Two SAPs with different radii, r_1 and r_2 ($r_1 \neq r_2$), are asymmetrically located at two sides of the core with different distances d_1 and d_2 against the center ($d_1 \neq d_2$). The common center O of the core and the cladding is not on a line with centers of SAPs. There is a misalignment angle ϑ in

the fiber sandwiched by two dotted lines (x_1 and x_2), which link the center of the fiber to centers of SAPs, respectively. The plane strain problem for the SIB in PMFs can be solved using a polar coordinate system and the result can then be transformed back to the rectangular coordinate system [7]-[14]. For an imperfect fiber considered here, each SAP has its associated polar and rectangular coordinate systems. They are $\rho(\theta_1)$ and x_1Oy_1 for SAP-1, as well as $\rho(\theta_2)$ and x_2Oy_2 for SAP-2. The common pole of two polar coordinate systems and the common origin of two rectangular coordinate systems are located at the same point, O, which is the common center of the fiber core and the cladding. For a given polar radius ρ in the polar system about the core, there are two polar angles θ_1 and θ_2 as well as two polar radii ρ_1 and ρ_2 in the polar systems of SAP-1 and SAP-2, respectively. The polar angles provide the misalignment angle ϑ in the PMF by $\vartheta = \theta_2 - \theta_1$. For SAP-1, $+x_1$- and $+y_1$-axes of the rectangular coordinate system correspond to polar angles of $\theta_1 = 0$ and $\theta_1 = \pi/2$ respectively. Similarly, $+x_2$- and $+y_2$-axes correspond to polar angles of $\theta_2 = 0$ and $\theta_2 = \pi/2$, respectively, for SAP-2.

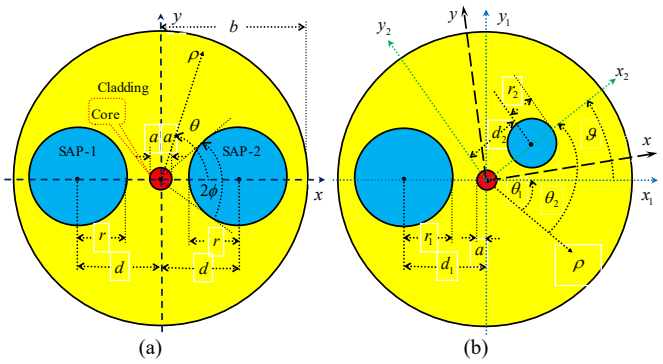

Fig. 1. The geometric structure and the coordinate systems of the Panda-type PMF with (a) symmetry and (b) asymmetry.

Following the classical stress analysis [15], at the center point O of the PMF, the principal stresses from SAP-1 are

$$\sigma_{x_1} = \sigma_{\rho_1}\Big|_{\theta_1=0}^{\rho_1=0} + \sigma_{\theta_1}\Big|_{\theta_1=\pi/2}^{\rho_1=0}; \quad \sigma_{y_1} = \sigma_{\rho_1}\Big|_{\theta_1=\pi/2}^{\rho_1=0} + \sigma_{\theta_1}\Big|_{\theta_1=0}^{\rho_1=0} \tag{1}$$

in the rectangular coordinate system of SAP-1, x_1Oy_1; and the principal stresses produced by SAP-2 are

$$\sigma_{x_2} = \sigma_{\rho_2}\Big|_{\theta_2=0}^{\rho_2=0} + \sigma_{\theta_2}\Big|_{\theta_2=\pi/2}^{\rho_2=0}; \quad \sigma_{y_2} = \sigma_{\rho_2}\Big|_{\theta_2=\pi/2}^{\rho_2=0} + \sigma_{\theta_2}\Big|_{\theta_2=0}^{\rho_2=0} \tag{2}$$

in the rectangular coordinate system of SAP-2, x_2Oy_2. The principal stresses from both SAPs in the rectangular coordinate system of the fiber, xOy, are

$$\begin{aligned} \sigma_x &= \sqrt{\sigma_{x_1}^2 + \sigma_{x_2}^2 + 2\sigma_{x_1}\sigma_{x_2}\cos\vartheta} \\ \sigma_y &= \sqrt{\sigma_{y_1}^2 + \sigma_{y_2}^2 + 2\sigma_{y_1}\sigma_{y_2}\cos\vartheta} \end{aligned}. \tag{3}$$

Then the SIB can be calculated from the difference between the principal stresses under the stress-optic coefficient C as $B = C(\sigma_x - \sigma_y)$, i.e.,

$$B = C\begin{pmatrix} \sqrt{\sigma_{x_1}^2 + \sigma_{x_2}^2 + 2\sigma_{x_1}\sigma_{x_2}\cos\vartheta} \\ -\sqrt{\sigma_{y_1}^2 + \sigma_{y_2}^2 + 2\sigma_{y_1}\sigma_{y_2}\cos\vartheta} \end{pmatrix}. \tag{4}$$

It achieves maximum $B_{\max} = C[(\sigma_{x_1} + \sigma_{x_2}) - (\sigma_{y_1} + \sigma_{y_2})]$ when $\vartheta = 0^\circ$. The minimum $B_{\min} = C(\sqrt{\sigma_{x_1}^2 + \sigma_{x_2}^2} - \sqrt{\sigma_{y_1}^2 + \sigma_{y_2}^2})$ occurs when $\vartheta = 90^\circ$. When there is only one SAP, or it is a single-hole PMF [14], the birefringence is $B = C(\sigma_x - \sigma_y)$. Eq. (4) provides the SIB in PMFs with the appropriated stress components σ_x and σ_y in Eq. (3), which exactly solves the disagreement between [7] and [8]. There are four instead of two stress components in the polar system contributing to the two principal stresses in the rectangular coordinate system. With this clarification, the SIB can be estimated using the stress components in corresponding polar coordinates based on the work in [8] as follows.

The total TEDP φ of the fiber transverse cross section includes the contribution φ_0 from the core, the contribution φ_1 from SAP-1, and the contribution φ_2 from SAP-2:

$$\varphi = \varphi_0 + \varphi_1 + \varphi_2 = \sum_{i=0}^{2}\varphi_i. \tag{5}$$

Three components in Eq. (9) satisfy the Poisson's equation

$$\nabla^2\varphi_i = \frac{1+\nu}{1-\nu}\Delta\alpha_i\Delta T_i \tag{6}$$

within their respective regions, where ν denotes the constant Poisson's ratio of the fiber glass, $\Delta\alpha_i$ represents the difference between the CTE in the considered region and that in the surrounding materials, ΔT is the difference between the melting temperature of the considered region and the room temperature, and the subscript i denotes 0 for the core, 1 for SAP-1, and 2 for SAP-2.

Meanwhile, three terms of the potential satisfy the Laplace's condition:

$$\nabla^2\varphi_i = 0 \tag{7}$$

outside their respective regions. Then the potential due to the area i are

$$\varphi_i^{\text{inside}} = \frac{\gamma}{4}\Delta\alpha_i\Delta T_i\rho_i^2 + K_i^{\text{inside}} \tag{8}$$

inside the area, where ρ_i is the radius vector in the polar coordinate system, K_i^{outside} are constants. The potential produced by the area i are

$$\varphi_i^{\text{outside}} = \frac{\gamma}{2}r_i^2\Delta\alpha_i\Delta T_i\ln\rho_i + K_i^{\text{outside}} \tag{9}$$

outside the area, where K_i^{outside} are constants again. Note there are $\rho_1 = \rho^2 - 2\rho r_1\cos\theta_1 + r_1^2$ and $\rho_2 = \rho^2 + 2\rho r_2\cos\theta_2 + r_2^2$.

On the other hand, the Airy stress function (ASF) F for the homogeneous part of the PMF is described as

$$F(\rho,\theta) = b_0\rho^2 + a_0 + \sum_{n=1}^{\infty}\left(a_n\rho^n + b_n\rho^{n+2}\right)\cos(n\theta) \tag{10}$$

where coefficients b_0, a_0, a_n and b_n are determined from the boundary conditions, and n is a integer $n = 1,2,3,4\ldots$. Then the

sum of the TEDP φ and the ASF F is given by $\xi = \varphi + F$, which describes the transversal stress state of the PMF. Stress components in the polar coordinate system are given by [7, 8]

$$\sigma_\rho = \frac{-E}{1+\nu}\frac{1}{\rho}\left(\frac{\partial \xi}{\partial \rho} + \frac{1}{\rho}\frac{\partial^2 \xi}{\partial \theta^2}\right), \tag{11}$$

$$\sigma_\theta = \frac{-E}{1+\nu}\frac{\partial \xi}{\partial \rho^2}, \tag{12}$$

$$\sigma_{\rho\theta} = \frac{-E}{1+\nu}\frac{\partial}{\partial \rho}\left(\frac{1}{\rho}\frac{\partial \xi}{\partial \theta}\right), \tag{13}$$

where E is the Young's modulus of the fiber which is assumed to be a constant across the transverse of the PMF. Then stress components can be obtained as

$$\sigma_{\rho_1}\Big|_{\theta_1=0}^{\rho_1=0} = \frac{-E}{1-\nu}\left[\frac{\Delta\alpha_0\Delta T_0}{2} + \frac{\Delta\alpha_s\Delta T_s}{2}\left(\frac{r_1}{d_1}\right)^2 + 2b_0\right], \tag{14}$$

$$\sigma_{\theta_1}\Big|_{\theta_1=0}^{\rho_1=0} = \frac{-E}{1-\nu}\left[\frac{\Delta\alpha_0\Delta T_0}{2} - \frac{\Delta\alpha_s\Delta T_s}{2}\left(\frac{r_1}{d_1}\right)^2 + 2b_0\right], \tag{15}$$

for SAP-1, and

$$\sigma_{\rho_2}\Big|_{\theta_2=0}^{\rho_2=0} = \frac{-E}{1-\nu}\left[\frac{\Delta\alpha_0\Delta T_0}{2} + \frac{\Delta\alpha_s\Delta T_s}{2}\left(\frac{r_2}{d_2}\right)^2 + 2b_0\right], \tag{16}$$

$$\sigma_{\theta_2}\Big|_{\theta_2=0}^{\rho_2=0} = \frac{-E}{1-\nu}\left[\frac{\Delta\alpha_0\Delta T_0}{2} - \frac{\Delta\alpha_s\Delta T_s}{2}\left(\frac{r_2}{d_2}\right)^2 + 2b_0\right], \tag{17}$$

for SAP-2. It is noted that b_0 from the ASF is crucial for the stress calculation according to [8], but is negligible for calculating the stress difference since it can be removed via a subtraction. In a similar way, it can be demonstrated that the difference in CTEs $\Delta\alpha_c$ and the difference in temperatures ΔT_c between those values in the cladding and the core, respectively, will not change the birefringence either. $\Delta\alpha_s$ and ΔT_s, the differences between those values in the cladding and SAPs will affect the stress difference and thereby the SIB. This is the same for both SAPs.

III. Numerical Simulations

The analytical expression of the SIB in asymmetric Panda-type PMFs can be obtained by substituting Eq. (14)-(17) into Eq. (4). The expression will cover all possible impacts from material and geometric parameters, especially from the misalign angle ϑ as shown in Fig. 2(a). The maximum birefringence occurs at a zero misalignment, $\vartheta = 0$, corresponding to the case of reflection symmetry about the x-axis [7], [8], The minimum birefringence occurs at $\vartheta = \pi$, corresponding to the case of a single SAP or a single-hole PMF [14]. The validity of the model can be proved by the agreement between the true SIB in practical PMFs and the calculated SIB, as listed in Table I and Fig.2(b). The true SIB is obtained from the experimental measurement of the beat length.

To compare our model with early works for symmetric -stress fibers, the SIB in Eq. (4) can be simplified as

$$B = \frac{-2CE\Delta\alpha_s\Delta T_s}{1-\nu}\left[\left(\frac{r_1}{d_1}\right)^2 + \left(\frac{r_2}{d_2}\right)^2\right]\cos\left(\frac{\vartheta}{2}\right), \tag{18}$$

since there are always a small misalign angle in practice, i.e., $\theta_1 \approx \theta_2$, then we have $\sigma_{x_1} \approx \sigma_{x_2}$, and $\sigma_{y_1} \approx \sigma_{y_2}$. Furthermore, it can be simplified as

$$B = \frac{-4CE\Delta\alpha_s\Delta T_s}{1-\nu}\left(\frac{r}{d}\right)^2 \tag{19}$$

for an ideal PMF, in which we have $\vartheta = 0$, $r = r_1 = r_2$, and $d = d_1 = d_2$. Calculations under same parameters according to Eq. (32) in [8] and Eq. (19) in [7] are shown in Fig. 2(c) and Fig. 2(d), respectively. It is found that, the periodic dependence of SIB on the polar angle and the (overestimated) magnitude reported in [8] was obviously incorrect. On the other hand, it is also clearly seen that results from [7] underestimated the SIB.

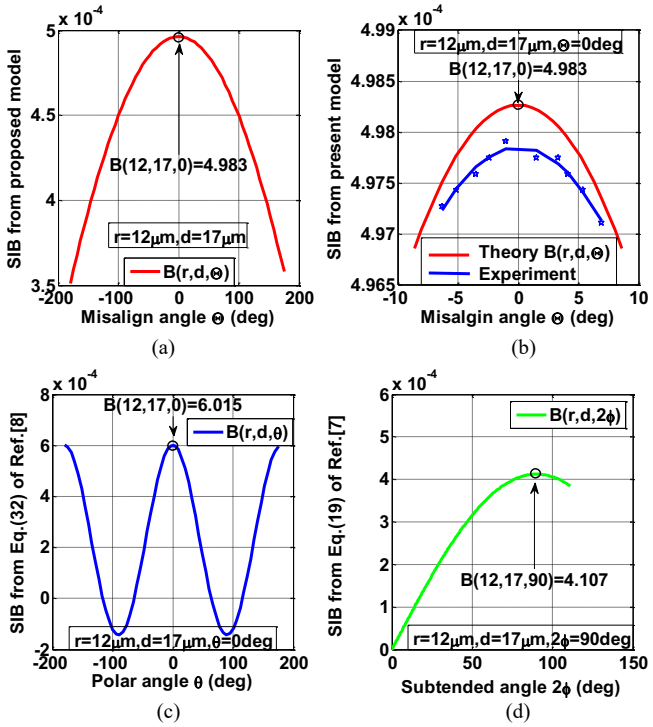

Fig. 2. SIB in Panda-type PMFs from (a) proposed model as a function of the misalignment angle between SAPs, (b) proposed model with measurement data at a small angle, (c) reported overestimation model in [8], and (d) reported underestimation model in [7].

TABLE I
Measurement Data for Practical Panda-Type PMFs

Misalign angle (deg)	Beat length (mm)	True SIB from beat length	Calculated SIB from Eq. (18)
+6.9	3.118	4.9711×10^{-4}	4.9736×10^{-4}
-3.5	3.115	4.9759×10^{-4}	4.9803×10^{-4}
-1.0	3.113	4.9794×10^{-4}	4.9825×10^{-4}
+5.4	3.116	4.9743×10^{-4}	4.9771×10^{-4}
-2.4	3.114	4.9775×10^{-4}	4.9816×10^{-4}
-5.1	3.116	4.9743×10^{-4}	4.9777×10^{-4}
+1.5	3.114	4.9775×10^{-4}	4.9822×10^{-4}
+4.1	3.115	4.9759×10^{-4}	4.9795×10^{-4}
-6.3	3.117	4.9727×10^{-4}	4.9751×10^{-4}
+3.3	3.114	4.9775×10^{-4}	4.9806×10^{-4}

The monotonic dependence of the SIB on the geometric parameters of SAPs (their radii r and distances d to the core) calculated by Eq. (18) are shown in Fig. 3(a) and Fig. 3(b). The results from [8] and [7] are shown in Fig. 3(c)/(d), and Fig. 3 (e)/(f), respectively. Only the trends of the dependence on distance are same, while the values differ by several times. Parameters of the PMF used in numerical estimations are the same: stress-optic coefficient $C = 3.36\times10^{-12}$ /Pa at the wavelength $\lambda = 1{,}550$ nm, the core radius $a = 3\times10^{-6}$ m, the cladding radius $b = 4\times10^{-5}$ m, the Poisson's ratio $v = 0.186$, the Young's modulus $E = 7.83\times10^{10}$ Pa, the difference of CTEs $\Delta\alpha_0 = 1.585\times10^{-6}$/K, $\Delta\alpha_s = 0.91\times10^{-6}$/K, and the difference of melting temperatures $\Delta T_0 = \Delta T_s = -850$ K between those values in the cladding and SAPs, respectively.

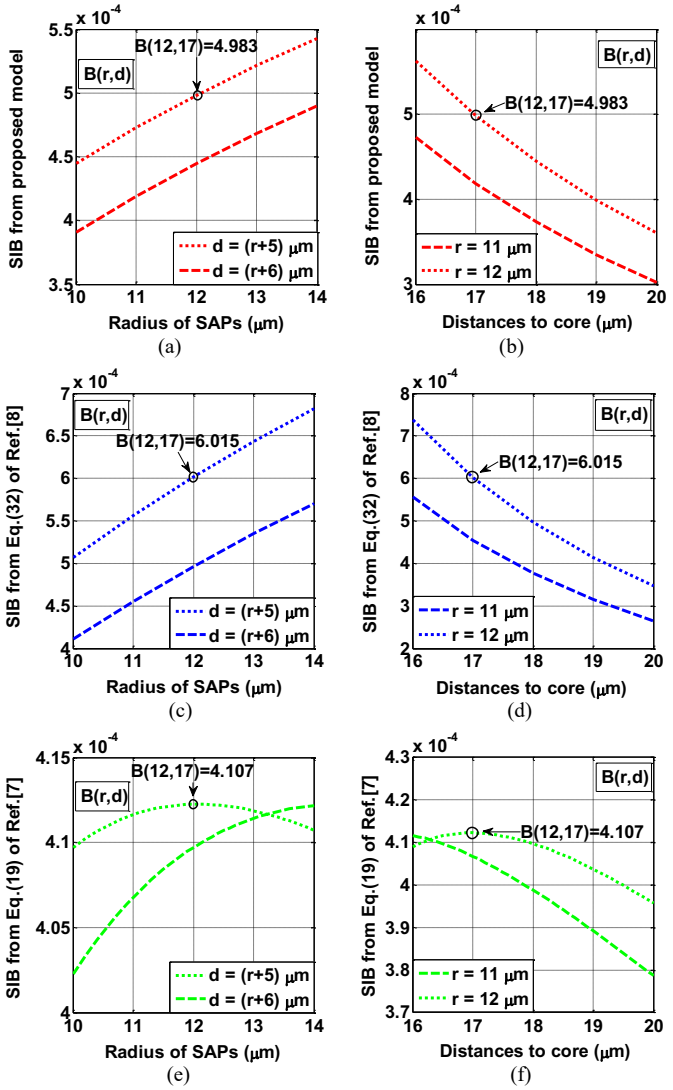

Fig. 3. SIB as functions of radius/distances of SAPs from (a)/(b) in proposed model, (c)/(d) reported overestimation model in [8], and (e)/(f) reported underestimation model in [7].

The result in Eq. (19) indicates that the two-fold symmetry (reflection symmetry about both x -axis and y -axis simultaneously) in ideal PMFs leads to the occurrence of the theoretical maximum at $\vartheta = 0$ and $r = (b-a)/2$ and $d = (b+a)/2$. This provides a theoretical upper limit of the SIB in ideal Panda-type PMFs, which is $B_{\max} = [-4CE\Delta\alpha_s\Delta T_s/(1-v)][(b-a)^2/(b+a)^2]$. Considering the mechanical reliability of a fiber, reasonable values can be chosen as $r = (b-2a)/2$ and $d = b/2$ for a more practical value of the SIB, which is $B_{\text{opt}} = [-4CE\Delta\alpha_s\Delta T_s/(1-v)](1-2a/b)^2$. From above analyses, our model provides a simpler and more accurate estimation of the SIB in the design and evaluation of PMFs.

IV. Conclusions

An analytical model of the stress-induced birefringence in Panda-type PMFs has been developed to provide a simpler and more accurate estimation for the SIB. It can be found that, the SIB in Panda-type PMFs highly depends on the geometric parameters of SAPs. It periodically depends on the misalignment angle between two SAPs, and also monotonically depends on the radii of the core and SAPs as well as the distances between the core and SAPs. For ideal PMFs, the periodic dependence of the SIB on the misalignment angle will disappear while its monotonic dependence on the radii and distances will still exist.

References

[1] F. Pang, H. Zheng, H. Liu, J. Yang, N. Chen, Y. Shang, S. Ramachandran, and T. Wang, "The orbital angular momentum fiber modes for magnetic field sensing," *Photon. Technol. Lett.*, vol. 31, no.11, pp. 893-896, 2019.

[2] D. Leandro and M. Lopez-Amo, "All-PM fiber loop mirror interferometer analysis and simultaneous measurement of temperature and mechanical vibration", *J. Lightwave Technol.*, vol. 36, no. 4, pp. 1105-1111, 2018.

[3] K. Sasaki, M. Takahashi, and Y. Hirata, "Temperature-insensitive Sagnac-type optical current transformer," *J. Lightwave Technol.*, vol. 33, No. 12, pp. 2463-2467, 2015.

[4] I. Abdulhalim, I. Gannot, and C. N. Pannell, "All-fiber and fiber compatible acousto-optic modulators with potential biomedical applacations," *Proc. SPIE*, vol. 6083, pp. 6830K, 2006.

[5] J. Liu, Y. Liu, and T. Xu, "Bias error and its thermal drift due to fiber birefringence in interferometric fiber-optic gyroscopes," *Opt. Fiber Technol.*, vol. 55, no. 3, pp. 102138, 2020.

[6] L. Zhao, Y. Zhang, Y. Chen, and J. Wang, "Simultaneous measurement of temperature and RI based on and optical microfiber coupler assembled by a polarization maintaining fiber," *App. Phys. Lett.*, vol. 114, pp. 151903, 2019.

[7] M. P. Varnham, David N. Payne, Arthur J. Barlow, and Robin D. Birch, "Analytic solution for the birefringence produced by thermal stress in polarization-maintaining optical fibers," *J. Lightwave Technol.*, vol. 1, no. 2, pp. 332-339, 1983.

[8] P. L. Chu and Rowland A. Sammut, "Analytical method for calculation of stresses and material birefringence in polarization-maintaining optical fiber," *J. Lightwave Technol.*, vol. 2, no. 5, pp. 650-662, 1984.

[9] R. H. Stolen, "Calculation of stress birefringence in fibers by an infinitesimal element method," *J. Lightwave Technol.*, vol. 1, no. 2, pp. 297-301, 1983.

[10] K. Okamoto, T. Hosaka, and T. Edahiro, "Stress analysis of optical fibers by a finite element method," *J. Quantum Electron,* vol. 17, no. 10, pp. 2123-2129, 1981.

[11] K. Hayata, M. Koshiba, and M. Cuzuki, "Vectorial wave analysis of stress-applied polarization-maintaining optical fiber by the finite-element method," *J. Lightwave Technol.,* vol. 4, no. 2, pp. 133-139, 1986.

[12] K. H. Tsai, K. S. Kim, and T. F. Morse, "General solutions for stress-induced polarization in optical fibers," *J. Lightwave Technol.*, vol. 9, no. 1, pp. 7-17, 1991.

[13] A. Kumar and A. Ghatak, *Polarization of Light with Applications in Optical Fibers*, SPIE Press, 2011, Chap.9, Birefringence in optical fibers: applications, pp.177-179.

[14] M. Karimi, F. Surre, Tons Sun, K. T. V. Grattan, W. Margulis, and P. Fonjallaz, "Theoretical analysis of a non-symmetric polarization-maintaining single-mode fiber for sensor applications," *J. Lightwave Technol.*, vol. 30, no. 3, pp. 362-367, 2012.

[15] S. Timoshenko and J. N. Goodier, *Theory of Elasticity*, 3rd edition, McGraw-Hill Book Company, Inc., 1970, Chap.4, Two-dimensional problems in polar-coordinates, pp. 55-58.

[16] R. Guan, F. Zhu, Z. Gan, D. H, and S. Liu, "Stress birefringence analysis of polarization maintaining optical fibers," *Opt. Fiber Technol.*, vol. 11, pp. 240-254, 2005.